

Vertebrobasilar Artery Geometry and Basilar Artery Plaques: A High-Resolution Magnetic Resonance Imaging Study

Jinmei Zheng

Fujian Medical University Union Hospital <https://orcid.org/0000-0002-2203-395X>

Bin Sun

Fujian Medical University Union Hospital

Ruolan Lin

Fujian Medical University Union Hospital

Yongqi Teng

Changle District Hospital of Fuzhou

Xihai Zhao

Tsinghua University School of Medicine

Yunjing Xue (✉ xueyunjing@126.com)

Fujian Medical University Union Hospital <https://orcid.org/0000-0003-4563-4763>

Research article

Keywords: Atherosclerosis, Intracranial arterial diseases, Magnetic resonance imaging, geometry, Vertebrobasilar

Posted Date: September 15th, 2020

DOI: <https://doi.org/10.21203/rs.3.rs-62822/v1>

License: © ⓘ This work is licensed under a Creative Commons Attribution 4.0 International License.

[Read Full License](#)

Abstract

Background

Atherosclerotic plaques are often present in regions with complicated flow patterns. Vascular morphology plays a role in hemodynamics. In this study, we investigate the relationship between the geometry of the vertebrobasilar artery system and the basilar artery (BA) plaque prevalence.

Methods

We enrolled 290 patients with posterior circulation ischemic stroke. We distinguished four configurations of the vertebrobasilar artery: Walking, Tuning Fork, Lambda, and No Confluence. The diameter of the vertebral artery (VA) and the number of bends in the intracranial VA segment was assessed using three-dimensional time-of-flight magnetic resonance angiography. We differentiated between multi-bending (≥ 3 bends) and oligo-bending (< 3 bends) VAs. High-resolution magnetic resonance imaging was used to evaluate BA plaques. Logistic regression models examined the relationship between the geometry type and BA plaque prevalence.

Results

After adjusting for sex, age, body mass index ≥ 28 , hypertension, and diabetes mellitus, the Walking, Lambda, and No Confluence geometries were associated with the presence of BA plaque. Patients with multi-bending VAs in both the Walking (71.43%, $P=0.003$) and Lambda group (40.43%, $P=0.018$) had more plaques compared to patients with oligo-bending VAs in these groups. In the Lambda group, the diameter difference between the VAs was larger in patients with BA plaques than that in patients without BA plaques (1.4 mm vs. 0.9 mm, $P<0.001$).

Conclusions

The Walking, Lambda, and No Confluence geometry, ≥ 3 bends in the VAs, and a large diameter difference between the VAs were associated with the presence of BA plaque.

Background

Intracranial atherosclerosis is an important cause of stroke worldwide [1] and accounts for almost 33–50% of ischemic strokes in the Chinese population [2]. Posterior circulation strokes account for about 20–30% of all ischemic strokes [3, 4], and vertebrobasilar atherosclerosis is a common cause of posterior circulation ischemic strokes.

Many conventional imaging modalities exist for identifying luminal stenosis, including digital subtraction angiography, computed tomography angiography, and three-dimensional time-of-flight magnetic resonance angiography (3D-TOF-MRA). However, identifying the morphology and composition of plaques has been shown to provide an incremental benefit over luminal stenosis alone when the aim is to define vulnerable lesions [5, 6] and predict subsequent cardiovascular ischemic events [7, 8], both in the coronary and carotid circulation. High-resolution magnetic resonance imaging (HRMRI) is a novel non-invasive technique to examine blood vessels and plaques, specifically cerebral vessel wall plaques [9]. Several recent studies have confirmed the feasibility of using HRMRI to evaluate intracranial arterial walls [9, 10]. However, most studies mainly focused on the relationship between plaque distribution, plaque enhancement, artery remodeling patterns, intraplaque hemorrhage, and clinical ischemic events [11–14]. There is limited research that investigates the association between the vascular geometry and the plaque prevalence in posterior circulation based on magnetic resonance imaging.

Atherosclerosis is not only associated with systemic risk factors such as hypertension, smoking, hyperlipidemia, and diabetes mellitus, but also focal vessel geometry [15]. The vertebrobasilar artery (VBA) system is unique in human anatomy in that two arteries (the left and right vertebral artery (VA)) merge into one artery (basilar artery (BA)). The diameters of the left and right VA differ in up to 50% of people [16], and their anatomical course is also different. Vertebrobasilar geometry can be classified into distinct configurations according to the anatomical course of the VA on either side and the difference in their diameters. Wake-Buck et al. [17] described the relationship between vertebrobasilar geometry and differences in hemodynamic distribution. Atherosclerotic plaques often develop in regions with low wall shear stress, such as the inner wall of a curved artery or the apex of a junction [18].

We hypothesized that different vertebrobasilar geometries with their specific hemodynamics will influence the presence of atherosclerotic plaques. This study aimed to explore a potential association between the presence of BA plaques and different vertebrobasilar geometries using HRMRI in vivo.

Material And Methods

Patients

We selected 303 consecutive patients who presented with a posterior circulation ischemic stroke to the Department of Neurology at our hospital between July 2017 and June 2018. Patients were included if they met the following criteria: (1) ischemic stroke or transient ischemic attack in the posterior circulation supplied by basilar artery presented with dizziness, unilateral limb weakness/ataxia, Gait ataxia and so on; (2) quality of the high-resolution magnetic resonance images sufficient for analysis. Our exclusion criteria were as follows: (1) nonatherosclerotic vasculopathy, such as dissection, arteritis or Moya-Moya disease; (2) evidence of a cardioembolic stroke (atrial fibrillation); (3) contraindications to MR imaging; (4) poor image quality due to motion artifact; (5) vascular geometry not classified. Based on these criteria, seven patients with motion artifacts, and six patients in whom vascular geometry could not be classified were excluded.

Eventually, 290 patients were enrolled in our study.

This study was approved by the local ethics committees, and all patients provided their written informed consent.

Imaging protocol

Patients were scanned with a 3.0 T MR imaging system (Discovery MR750, General Electric Medical System, Milwaukee, WI, USA). The imaging protocols included T1-weighted imaging (T1WI), T2-weighted imaging (T2WI), diffusion-weighted imaging, 3D-TOF-MRA, and three-dimensional fast-spin-echo T1-weighted sequence (CUBE). The parameters of 3D-TOF-MRA were set as follows: TR/TE = 19/3.5 ms, FOV = 180 mm × 180 mm, slice thickness = 1.2 mm, matrix = 288 × 288, bandwidth = 31.25 Hz, number of excitations = 1, the spatial resolution is 0.625 × 0.625 × 1.2 mm, acquisition time = 5 min 45 s. The CUBE parameters were as follows: TR/TE = 600/16.5 ms, FOV = 180 mm × 180 mm, slice thickness = 0.8 mm, matrix = 288 × 288, bandwidth = 50 Hz, number of excitations = 2, ETL = 30, phase acceleration = 1.75, the spatial resolution is 0.625 × 0.625 × 0.8 mm, a slab-selective excitation was used, the coronal scanning coverage was from the basilar artery to the intracranial segment of vertebral arteries and the anterior circulation was not covered, acquisition time = 6 min 46 s. The coronal CUBE images were transferred to a local postprocessing station (Advantage Workstation, AW 4.5; General Electric Medical System, Milwaukee, WI, USA), and axial CUBE images were reformatted with sequential 1 mm intervals.

Image analysis

A plaque was defined as an eccentric wall thickening, whereas the thinnest part was estimated to be < 50% of the thickest part by visual inspection on axial CUBE images [19] (Fig. 1). The presence or absence of BA plaque was reviewed by two experienced readers (Zheng and Xue) blinded to MRA findings. The differences between the two observers were solved by consensus. To assess intra-observer reproducibility, CUBE images were reevaluated by one reviewer (Zheng) one month later.

The diameter of the VA was measured on 3D-TOF-MRA. The diameter of each vessel was calculated as the average of the measurements made at three consecutive points, 3 mm apart, starting from the vertebrobasilar junction (for both VAs and the BA) [16, 20]. The dominant VA was defined as: the diameter of the VA on the dominant side was wider than that of the contralateral VA (difference in diameter \geq 0.3 mm) [16, 20].

Based on the 3D-TOF-MRA images, VBA geometry was qualitatively classified into four basic geometric configurations: Walking, Tuning Fork, Lambda, and No Confluence (Fig. 2). The Walking geometry is distinguished by two VAs with a diameter difference of less than 0.3 mm that bend in the same direction before merging into the BA [16, 17]. The Tuning Fork shows two VAs of equal diameter (difference in diameter < 0.3 mm) that bend in opposite directions to form a symmetrical confluence from which the BA emerges [16, 17]. The Lambda geometry is defined as two VAs with a diameter difference of at least 0.3 mm that merge into the BA [16, 17]. In the No Confluence configuration, the VAs are not merged, but

one VA continues as the BA, and the other VA feeds into other arteries, mostly the posterior inferior cerebellar artery.

Vertebral artery limited by posterior fossa bends mainly to left or right, the number of bends in the intracranial segments of the VAs was assessed on 3D-TOF-MRA images. Two 5 mm long lines were drawn starting from the vertex of a vascular curve to both sides, which intersect with the VA to form an angle. If this angle was $\leq 150^\circ$, it was defined as a vascular bend (Fig. 3). According to the total number of bends in the VAs' intracranial segments, patients were divided into a multi-bending group (total number of bends ≥ 3) and an oligo-bending group (total number of bends < 3). Vascular curvature was measured by the same two observers (Zheng and Xue) one month later blinded to HRMRI findings. We took the consensus results from the measurements of two radiologists. To assess intra-observer reproducibility, vascular curvature was remeasured by one reviewer (Zheng) one month later.

Statistical analysis

Quantitative data were expressed as the mean \pm standard deviation (SD), and qualitative data were expressed as percentages. The Shapiro-Wilk test for normality was used to investigate the distribution of data. Intraobserver or interobserver variability for the identification of BA plaque and vascular curvature measurements was performed using the intraclass correlation coefficient (ICC) analysis. The comparison of the BA plaque prevalence in the four different vascular geometries was performed using the chi-square test. Logistic regression models further examined the relationship between the geometry type and BA plaque prevalence. The comparison between multi-bending and oligo-bending VAs was performed by the chi-square and Fisher exact test. In the case of the Lambda configuration, differences in the diameter between the right and left VA for patients with and without BA plaques were compared with the Mann-Whitney U test, and a receiver operating characteristic curve analysis was used to identify the best cutoff value correlated with the presence of BA plaque. A *P*-value < 0.05 was considered to be statistically significant.

The statistical analysis was performed using IBM SPSS Statistics for Windows, version 19.0 (IBM Corp., Armonk, NY, USA).

Results

The clinical characteristics of the study population are summarized in Table 1.

The mean age of the 290 patients was 68.5 ± 10.3 years, and 60% were males. A total of 86 patients (mean age, 70.2 ± 10.6 years) had BA plaques, and 204 patients (mean age, 67.7 ± 10.1 years) had no BA plaques. A body mass index ≥ 28 , hypertension, and diabetes mellitus were more frequent in patients with BA plaques as compared to patients without BA plaques. The comparison of clinical risk factors between patients with and without BA plaques is shown in Table 2. Based on their VBA geometry, 49 patients were assigned to the Walking group, 73 patients were in the Tuning group, 144 patients were classified into the Lambda group, and the last 24 patients belong to No Confluence group.

The inter-observer and intra-observer reproducibility for identification of BA plaque were ICC = 0.905 (95% CI 0.779–0.961) and ICC = 0.903 (95%CI 0.774–0.960), respectively. The inter-observer and intra-observer reproducibility for vascular curvature measurement were ICC = 0.905(95% CI 0.778–0.961) and ICC = 0.883(95%CI 0.728–0.952), respectively.

Table 1
Clinical Characteristics of the Study Population (n = 290)

	Mean ± SD or n(%)
Sex, male	174(60.0)
Age, y	68.5 ± 10.3
Smoking	103(35.52)
BMI ≥ 28	39(13.45)
Hypertension	203(70.00)
Diabetes mellitus	101(34.83)
Hyperlipidemia	118(40.69)
Coronary heart disease	36(12.41)
Values are presented as mean ± standard deviation or number (%); BMI, body mass index.	

Table 2
Comparison of Clinical Risk Factors between BA with and without Plaque.

	BA plaque (+)(N = 86)	BA plaque (-)(N = 204)	<i>P</i>
Sex, male	50(58.14)	124(60.78)	0.675
Age, y	70.2 ± 10.6	67.7 ± 10.1	0.064
BMI ≥ 28	17(19.77)	22(10.78)	0.041
Smoking	29(33.72)	74(36.27)	0.678
Hypertension	69(80.23)	134(65.69)	0.014
DM	39(45.35)	62(30.39)	0.015
Hyperlipidemia	38(44.19)	80(39.22)	0.431
CHD	11(12.79)	25(12.25)	0.899
Values are presented as mean ± standard deviation or number (%); BMI, body mass index; DM, diabetes mellitus; CHD, coronary heart disease; BA, basilar artery.			

Correlation between VBA geometry and the presence of BA plaque

The BA plaque prevalence was highest in patients who had a Walking configuration (53.06%) and lowest in patients with a Tuning Fork configuration (15.07%). There was a significant difference in the BA plaque prevalence among the four basic geometric configurations ($\chi^2 = 21.265$, $P < 0.001$, Table 3).

Table 4 shows the association between VBA geometry and BA plaques. In the binary logistic regression analysis, Walking (odds ratio, 6.372; 95% confidence interval, 2.718–14.937; $P < 0.001$), Lambda (odds ratio, 2.168; 95% confidence interval, 1.037–4.533; $P = 0.04$), and No Confluence configuration (odds ratio, 3.382; 95% confidence interval, 1.188–9.625; $P = 0.022$) were found to be significantly associated with presence of BA plaque. After adjusting for age, sex, body mass index > 28, hypertension, and diabetes mellitus, these associations remained statistically significant (all $P < 0.05$; Table 4).

Table 3
Comparison of BA Plaque Prevalence in the four Geometric Configurations

VBA geometry	BA plaque (+)(N = 86)	BA plaque (-)(N = 204)	<i>P</i>
			0.001
Walking(49)	26(53.06)	23(46.94)	
Tuning Fork(73)	11(15.07)	62(84.93)	
Lambda(144)	40(27.78)	104(72.22)	
No Confluence(24)	9(37.50)	15(62.50)	
Values are presented as number (%);BA, basilar artery; VBA, vertebrobasilar artery;			

Walking VS Tuning Fork, $P \leq 0.001$; Walking VS Lambda, $P = 0.001$; Walking VS No Confluence, $P = 0.211$; Tuning Fork VS Lambda, $P = 0.037$; Tuning Fork VS No Confluence, $P = 0.018$; Lambda VS No Confluence, $P = 0.332$; and $P = 0.007$ considered to be statistically significant.

Table 4
Association between VBA Geometry and BA Plaque.

	Model 0		Model 1	
VBA geometry	OR(95% CI)	<i>P</i> Value	OR(95% CI)	<i>P</i> Value
Tuning Fork	reference		reference	
Walking	6.372(2.718–14.937)	0.001	6.792(2.805–16.447)	0.001
Lambda	2.168(1.037–4.533)	0.04	2.420(1.131–5.179)	0.023
No Confluence	3.382(1.188–9.625)	0.022	3.502(1.179–10.406)	0.024

OR, odds ratio; CI, confidence interval; Model 0: no adjustment has been done; Model 1: adjust for sex, age, BMI \geq 28, hypertension, and Diabetes mellitus.

Correlation between the number of vascular bends and the presence of BA plaque

In the Walking group, patients with multi-bending VAs had a higher BA plaque prevalence than patients with oligo-bending VAs (71.43% vs. 28.57%, respectively; $\chi^2 = 8.849$, $P = 0.003$). In the Lambda group, patients with multi-bending VAs had a higher BA plaque prevalence compared with patients with oligo-bending VAs (40.43% vs. 21.65%, respectively; $\chi^2 = 5.563$, $P = 0.018$). In the Tuning Fork group, none of the four patients with multi-bending VAs had BA plaques. In the No Confluence group, all patients had oligo-bending VAs (Table 5), and 9 patients (37.5%) of them had BA plaques.

Table 5
Comparison of Bending Number in the bilateral VAs' Intracranial Segments between Patients with and without BA Plaque

	BA plaque (+)(N = 86)	BA plaque (-)(N = 204)	<i>P</i>
Walking(49)			0.003
Multi-bending	20(71.43%)	8(28.57%)	
Oligo-bending	6(28.57%)	15(71.43%)	
Tuning Fork(73)			1.000
Multi-bending	0	4	
Oligo-bending	11(15.94%)	58(84.06%)	
Lambda(144)			0.018
Multi-bending	19(40.43%)	28(59.57%)	
Oligo-bending	21(21.65%)	76(78.35%)	
No Confluence(24)			–
Multi-bending	0	0	
Oligo-bending	9	15	
Values are presented as number (%); BA, basilar artery; VA, vertebral artery.			

Correlation between VA diameter difference and the presence of BA plaque

Twenty-four of the 290 patients (8.3%) had a No Confluence configuration. In the 266 patients with either Walking, Tuning Fork, or Lambda, the average diameter of the left VA was 2.67 mm \pm 0.64 mm and of the right, VA was 2.47 mm \pm 0.58 mm ($P < 0.001$). The diameters of the right and left VA were of equal size in

122 patients (45.86%). Among the remaining 144 patients, left VA dominance was identified in 95 (65.97%) and right VA dominance in 49 (34.03%) patients.

In the Lambda group, the mean diameter difference between the VAs was 1.4 mm (0.9 mm -1.6 mm) in patients with BA plaques and 0.9 mm (0.6 mm-1.3 mm) in patients without BA plaques ($P < 0.001$). The receiver operating characteristic curve analysis identified a cutoff value for the difference in VA diameter related to BA plaque formation of 1.35 mm.

Discussion

This study investigated the relationship between VBA geometry and BA plaque prevalence. We found that BA plaque prevalence was highest in the Walking geometry (53.06%) and lowest in the Tuning Fork geometry (15.07%). Moreover, the number of vascular bends in the intracranial segments of the VAs and the difference in diameter between the right and left VA also affected the presence of BA plaque.

Yu et al. [16] have investigated the relationship between the geometry patterns of vertebrobasilar artery and atherosclerosis. In their study, the vertebrobasilar artery geometry was qualitatively classified into four basic configurations: Walking, Tuning, Dominant-Lambda, and Hypoplasia-Lambda. They didn't focus on the No Confluence Geometry, which plays an important role in the presence of BA plaque. However, in their study, they only explored the correlation between the geometric configurations and BA plaque distribution. In the present study, we investigated the relationship between the geometry of the vertebrobasilar artery system and the presence of BA plaque. In the future study, we also want to determine the relationship between geometric configurations (Walking, Tuning Fork, Lambda, and No Confluence) and the distribution of BA plaque. Besides, in the Yu et al's study, 84 patients were included in the final analysis. In contrast, our study recruited 290 patients in the final analysis which will increase the power of statistical analysis.

Ravensbergen et al. [18, 21, 22] in their studies employed autopsy and a series of junction models, and demonstrated that vertebrobasilar geometry affects hemodynamics and that atherosclerotic plaques are often found in regions with complex flow patterns and/or low wall shear stress. In the previous study [17] high-field MRI was used in conjunction with computational fluid dynamics (CFD) modeling to investigate the hemodynamics of subject-specific confluence models ($n = 5$, two with Walking, two with Tuning Fork, and one with Dominant-Lambda geometry), and showed that vertebrobasilar geometry strongly influences both the skewing of velocity profiles and wall shear stress distribution in the VBA system. In Walking geometry, the BA flow resulting from the merging of two VAs that bend in the same direction (right) makes the BA flow curve to the opposite direction (left). These chronic processes may induce a BA curvature. The shear stress is low at the inner wall of the BA curvature, and atherosclerotic plaques are prone to form in regions with low shear stress. Also, in the Walking geometry, the BA flow resulting from the VA flows swirling upward makes the flow distribution more complex, which can also induce plaque formation [17]. In the Tuning Fork geometry, the flows in the BA are roughly parallel, and the velocity

profile peak in the BA is rather central [17], resulting in the low BA plaque prevalence in this geometric configuration.

In our study, BA plaque prevalence in the Lambda configuration (27.78%) was higher than that in the Tuning Fork configuration (15.07%). Compared to Lambda patients without BA plaques, those with BA plaques had a larger difference in the diameters of their VAs. In a study by Hong et al. [20] BA curvature was found to be associated with a diameter difference between the VAs. The BA flow resulting from VAs with a diameter difference ≥ 0.3 mm makes the BA flow curve to the side of the weaker VA, and the chronic processes caused by the asymmetric VA flow induce greater curving of the BA wall, which consequently may cause atherogenesis.

We found that BA plaque prevalence in the No Confluence geometry (37.50%) was also higher than that in the Tuning Fork geometry (15.07%). We hypothesize that BA flow coming from one VA also causes the BA flow curve to the wall opposite to the VA, and as a chronic process may consequently cause a curving of the BA wall. Subsequently, the deformation of the BA wall makes it prone to atherogenesis, which may lead to ischemic stroke in the posterior circulation. To date, there are no hemodynamic studies in patients with No Confluence geometry.

In our study, BA plaque prevalence was higher in patients with multi-bending VAs as compared to patients with oligo-bending VAs. We think that the flow patterns in the first group are more complex than that in the latter.

Our results have important clinical implications. First, we further classified VBA geometry based on the difference in diameter between the VAs and the VA course, which may help to improve the understanding of the vertebrobasilar system. Second, we demonstrated that the Walking, Lambda, and No Confluence geometry, multi-bending of the intracranial VA segment, and a large difference in the diameters of the VAs are high-risk factors for BA atherosclerosis initiation. Therefore, people with these geometric factors should be careful to prevent BA plaque formation.

Our study has several limitations. First, we did not measure the hemodynamics and flow distribution in the four geometric configurations. The underlying mechanism of the basilar artery geometry influencing the development of atherosclerotic plaques needs to be investigated from the hemodynamic aspect in future studies. Second, vascular curvature measurements were done manually from 2D images, since 2D had limited orientation, the vascular curvature at other dimensions cannot be assessed and the processing of vascular curvature measurements may be affected as the effect of flow artifact on 3D-TOF MRA. Third, coronal scanning was performed using the three-dimensional-CUBE sequence, and axial CUBE images were reconstructed. Wall thickness measurements from 3D MPR to determine plaque could be affected by volume averaging artifacts as the image resolution is comparable to the artery wall size, especially, when the basilar artery wall-thickening was not significant. Four, this is a pilot study with a limited sample size. Future studies recruiting larger populations are warranted. Five, even though a cut-off of 0.3 mm was used to define a dominant vertebral artery in previous studies (16,17), the spatial

resolution $0.625 \times 0.625 \times 1.2$ mm maybe was not high enough in this study. Finally, this study is an observational cross-sectional design, thus may be influenced by uncontrolled confounding.

Conclusion

In conclusion, this study explored the correlation between vertebrobasilar geometry and the presence of BA plaque. The BA plaque prevalence was highest in the Walking and lowest in the Tuning Fork configuration. Further, the extent of vascular bending in the intracranial VA segments and the diameter difference between the two VAs also were associated with the presence of BA plaque.

Abbreviations

BA, basilar artery

VA, vertebral artery

VBA, vertebrobasilar artery

3D-TOF-MRA, three-dimensional time-of-flight magnetic resonance angiography

HRMRI, high-resolution magnetic resonance imaging

Declarations

Ethics approval and consent to participate

The present study was approved by the Ethics Committee of Fujian Medical University Union Hospital, and all patients provided their written informed consent.

Consent for publication

Not applicable.

Availability of data and materials

The datasets used and/or analyzed during the current study are available from the corresponding author on reasonable request.

Competing interests

The authors declare that they have no competing interests.

Funding

This work was supported by the Joint Funds for the Innovation of Science and Technology, Fujian Province [Grant number:2018Y9025].

Authors' contribution

Jinmei Zheng analyzed the data, and wrote the original draft. Data collection were performed by Jinmei Zheng, Bin Sun, Ruolan Lin, and Yongqi Teng. Xihai Zhao analyzed the data, and edited the manuscript. Yunjing Xue supervised the whole study, and edited the manuscript. All authors read and approved the final manuscript.

Acknowledgments

Not applicable.

References

1. Gorelick PB, Wong KS, Bae H, Pandey DK. Large artery intracranial occlusive disease: a large worldwide burden but a relatively neglected frontier. *Stroke*. 2008;39:2396–9.
2. Wong LK. Global burden of intracranial atherosclerosis. *Int J Stroke*. 2006;1:158–9.
3. Amin-Hanjani S, Pandey DK, Rose-Finnell L, Du X, Richardson D, Thulborn KR, Elkind MS, Zipfel GJ, Liebeskind DS, Silver FL, Kasner SE, Aletich VA, Caplan LR, Derdeyn CP, Gorelick PB, Charbel FT. Vertebrobasilar Flow Evaluation and Risk of Transient Ischemic Attack and Stroke Study Group. Effect of Hemodynamics on Stroke Risk in Symptomatic Atherosclerotic Vertebrobasilar Occlusive Disease. *JAMA Neurol*. 2016;73:178–85.
4. Nouh A, Remke J, Ruland S. Ischemic posterior circulation stroke: a review of anatomy, clinical presentations, diagnosis, and current management. *Front Neurol*. 2014;5:1–16.
5. Underhill HR, Hatsukami TS, Fayad ZA, Fuster V, Yuan C. MRI of carotid atherosclerosis: clinical implications and future directions. *Nat Rev Cardiol*. 2010;7:165–73.
6. Garcia-Garcia HM, Costa MA, Serruys PW. Imaging of coronary atherosclerosis: intravascular ultrasound. *Eur Heart J*. 2010;31:2456–69.
7. Stone GW, Maehara A, Lansky AJ, de Bruyne B, Cristea E, Mintz GS, Mehran R, McPherson J, Farhat N, Marso SP, Parise H, Templin B, White R, Zhang Z, Serruys PW. PROSPECT Investigators. A prospective Natural History Study of Coronary Atherosclerosis. *N Engl J Med*. 2011;364:226–35.
8. Saam T, Hetterich H, Hoffmann V, Yuan C, Dichgans M, Poppert H, Koepfel T, Hoffmann U, Reiser MF, Bamberg F. Meta-analysis and systematic review of the predictive value of carotid plaque

- hemorrhage on cerebrovascular events by magnetic resonance imaging. *J Am Coll Cardiol.* 2013;62:1081–91.
9. Ryu CW, Jahng GH, Kim EJ, Choi WS, Yang DM. High resolution wall and lumen MRI of the middle cerebral arteries at 3 T. *Cerebrovasc Dis.* 2009;27:433–42.
 10. Li ML, Xu WH, Song L, Feng F, You H, Ni J, Gao S, Cui LY, Jin ZY. Atherosclerosis of middle cerebral artery: evaluation with high-resolution MR imaging at 3T. *Atherosclerosis.* 2009;204:447–52.
 11. Yu JH, Kwak HS, Chung GH, Hwang SB, Park MS, Park SH. Association of Intraplaque Hemorrhage and Acute Infarction in Patients With Basilar Artery Plaque. *Stroke.* 2015;46:2768–72.
 12. Wang W, Yang Q, Li D, Fan Z, Bi X, Du X, Wu F, Wu Y, Li K. Incremental Value of Plaque Enhancement in Patients with Moderate or Severe Basilar Artery Stenosis: 3.0 T High-Resolution Magnetic Resonance Study. *Biomed Res Int.* 2017;2017:4281629.
 13. Ma N, Jiang WJ, Lou X, Ma L, Du B, Cai JF, Zhao TQ. Arterial remodeling of advanced basilar atherosclerosis: a 3-teslar MRI study. *Neurology.* 2010;75:253–8.
 14. Yu J, Li ML, Xu YY, Wu SW, Lou M, Mu XT, Feng F, Gao S, Xu WH. Plaque distribution of low-grade basilar artery atherosclerosis and its clinical relevance. *BMC Neurol.* 2017;17:1–6.
 15. Malek AM, Alper SL, Izumo S. Hemodynamic shear stress and its role in atherosclerosis. *JAMA.* 1999;282:2035–42.
 16. Yu J, Zhang S, Li ML, Ma Y, Dong YR, Lou M, Feng F, Gao S, Wu SW, Xu WH. Relationship between the geometry patterns of vertebrobasilar artery and atherosclerosis. *BMC Neurol.* 2018;18:1–5.
 17. Wake-Buck AK, Gatenby JC, Gore JC. Hemodynamic characteristics of the vertebrobasilar system analyzed using MRI-based models. *PLoS One.* 2012;7:e51346.
 18. Ravensbergen J, Ravensbergen JW, Krijger JK, Hillen B, Hoogstraten HW. Localizing role of hemodynamics in atherosclerosis in several human vertebrobasilar junction geometries. *Arterioscler Thromb Vasc Biol.* 1998;18:708–16.
 19. Xu WH, Li ML, Gao S, Ni J, Zhou LX, Yao M, Peng B, Feng F, Jin ZY, Cui LY. Plaque distribution of stenotic middle cerebral artery and its clinical relevance. *Stroke.* 2011;42:2958–9.
 20. Hong JM, Chung CS, Bang OY, Yong SW, Joo IS, Hub K. Vertebral artery dominance contributes to basilar artery curvature and peri-vertebrobasilar junctional infarcts. *J Neurol Neurosurg Psychiatry.* 2009;80:1087–92.
 21. Ravensbergen J, Krijger JK, Verdaasdonk AL, Hillen B, Hoogstraten HW. The influence of the blunting of the apex on the flow in a vertebro-basilar junction model. *J Biomech Eng.* 1997;119:195–205.
 22. Ravensbergen J, Krijger JK, Hillen B, Hoogstraten HW. The influence of the Angle of confluence on the flow in a Vertebro basilar junction Modle. *J Biomech Eng.* 1996;29:281–99.

Figures

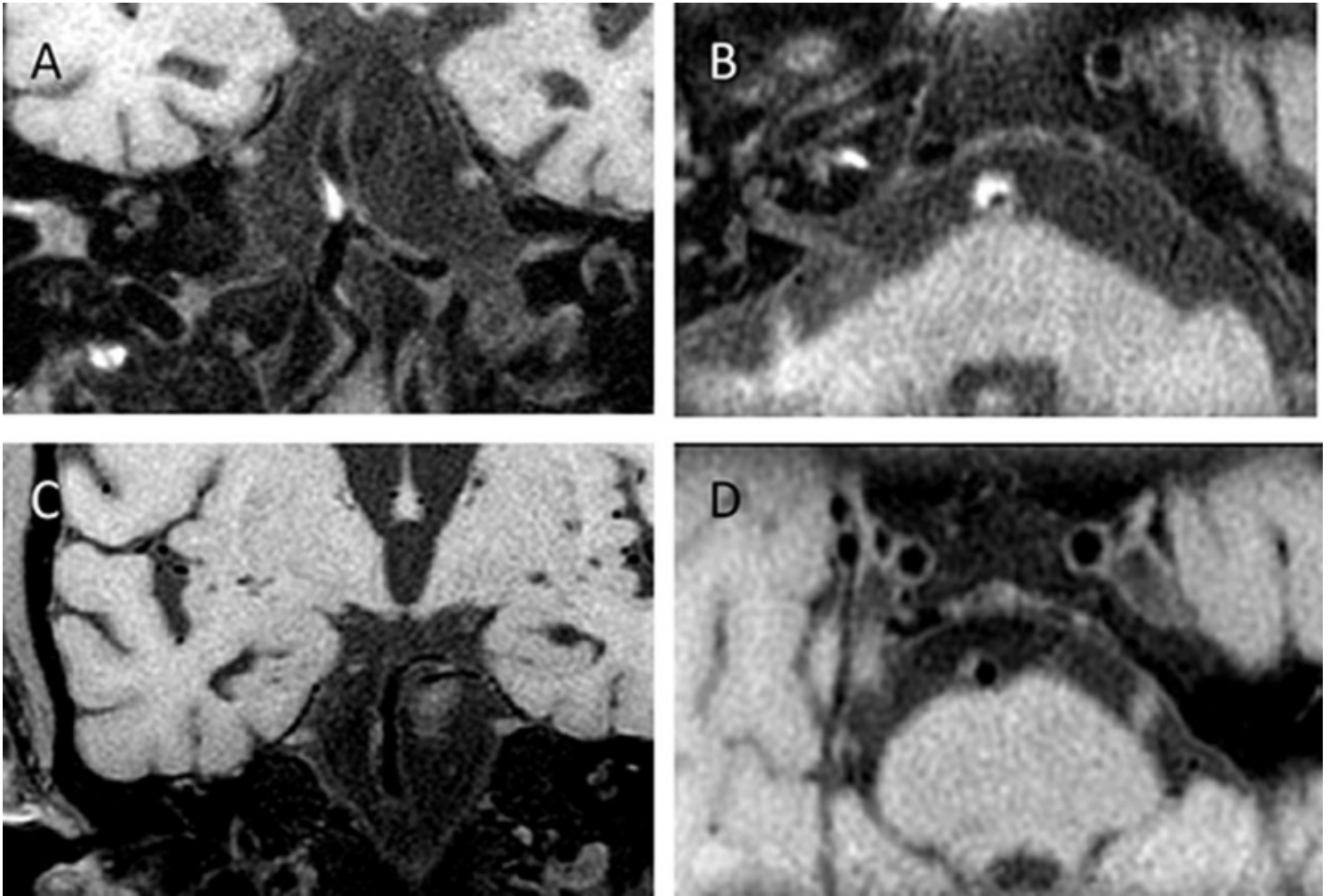


Figure 1

Example figures of plaques on 3D CUBE T1WI. An atherosclerotic plaque was present on coronal image (A) and corresponding reconstructed axial image(B) from a 79 years old male patient. Images C and D are from another male patient with 64 years old. An atherosclerotic plaque can be found on coronal image (C) and corresponding reconstructed axial image(D).

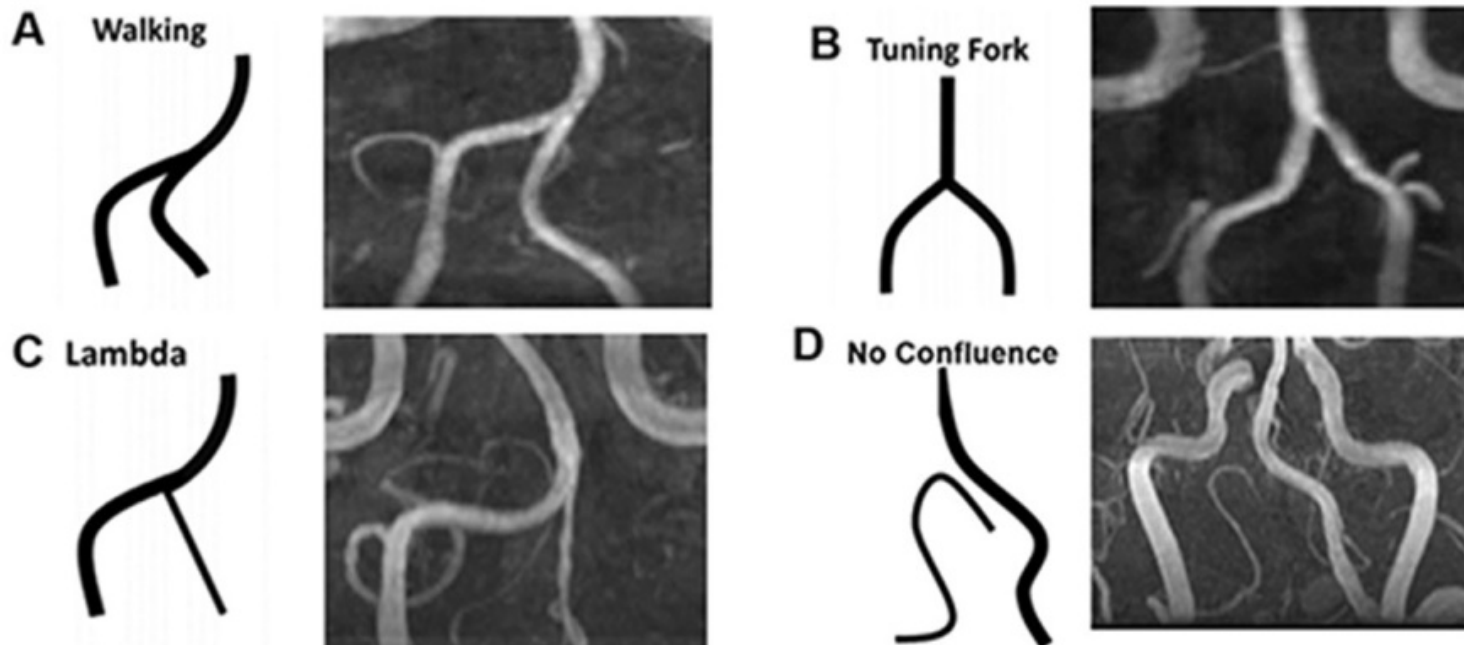


Figure 2

Examples for different geometry types of Vertebrobasilar artery system. The vertebrobasilar artery geometry is qualitatively classified into four basic geometric configurations: Walking (A), Tuning Fork (B), Lambda (C), and No Confluence (D). In each panel, a schematic of the configuration is followed by anterior-posterior magnetic resonance angiography.

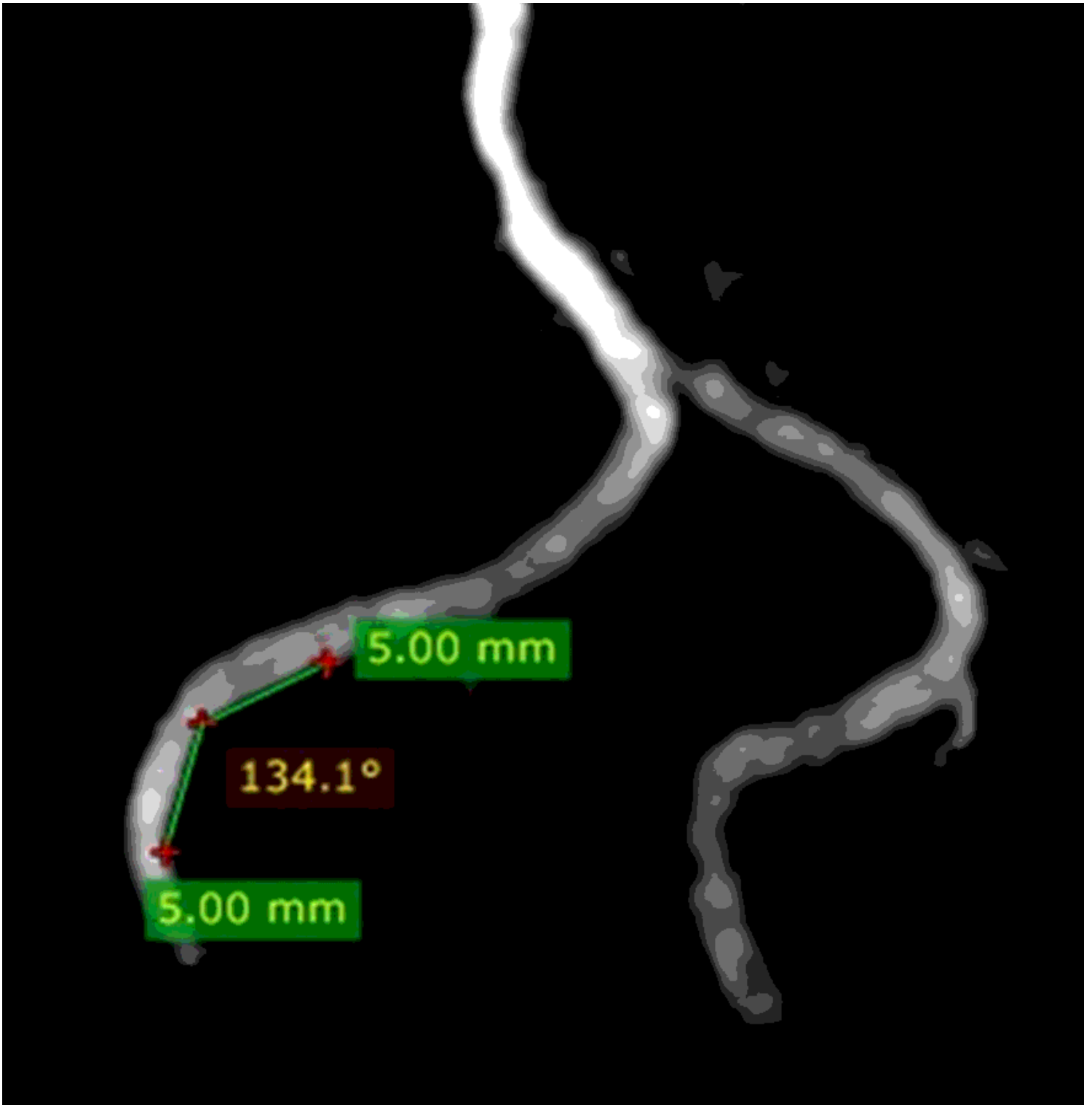


Figure 3

Schematic diagram of vascular curvature in vertebral artery. Two 5 mm long lines were drawn starting from the vertex of a vascular curve to both sides, the two lines intersect with the VA to form an angle. a vascular bend was identified If this angle was $\leq 150^\circ$